

Critical Interactions Between the SARS-CoV-2 Spike Glycoprotein and the Human ACE2

Receptor

Elhan Taka¹¶, Sema Z. Yilmaz¹¶, Mert Golcuk¹¶, Ceren Kilinc¹, Umut Aktas¹, Ahmet Yildiz^{2,3},

*Mert Gur¹**

¹ Department of Mechanical Engineering, Istanbul Technical University (ITU), Istanbul, Turkey

² Physics Department, University of California, Berkeley, CA, USA

³ Department of Molecular and Cellular Biology, University of California, Berkeley, CA, USA

*Corresponding author. Email address: gurme@itu.edu.tr

¶E.T., S.Z.Y., and M.G. (Mert Golcuk) contributed equally.

Supporting Information

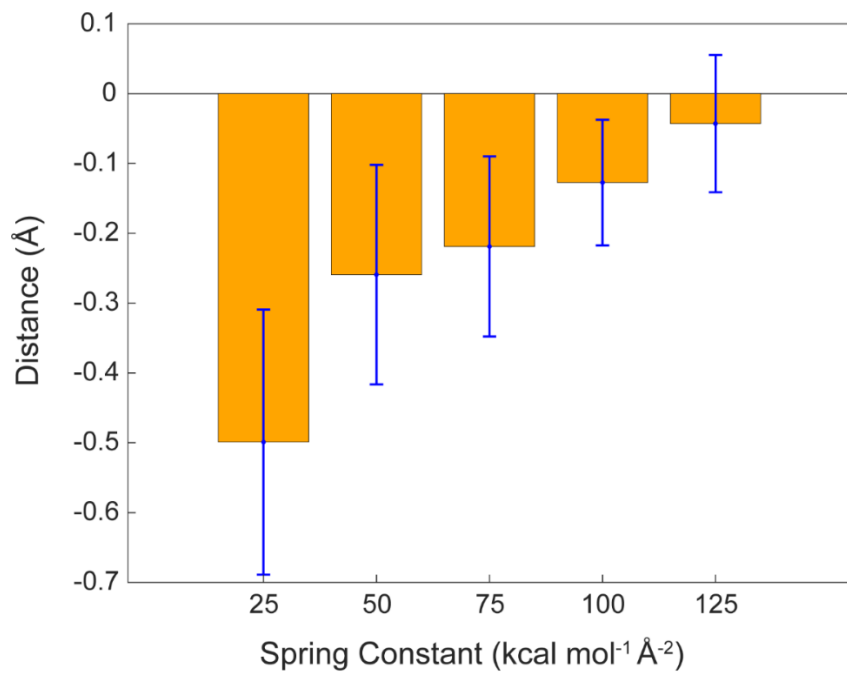


Figure S1. Distance between the dummy atom and steered atoms during SMD simulations. The average distance between the dummy atoms and the center of steered atoms are evaluated using all recorded conformations along each SMD simulations performed with spring constants of 25-125 $kcal\ mol^{-1}\ \text{\AA}^{-2}$.

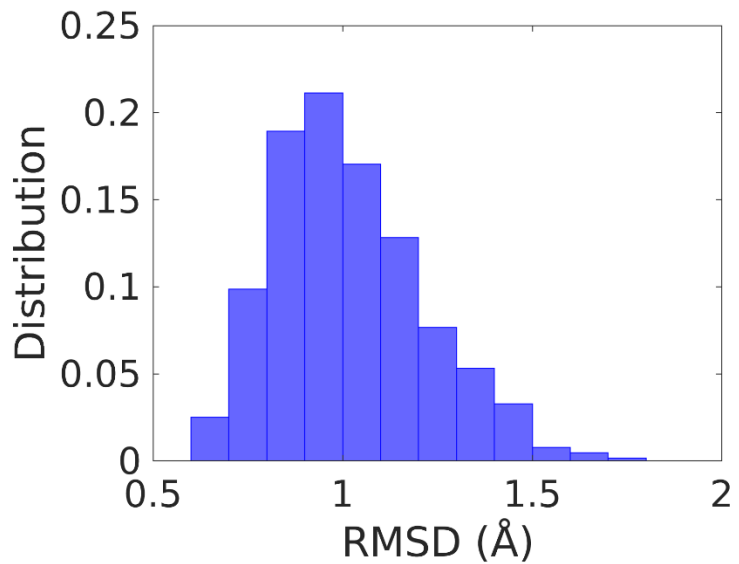


Figure S2. Normalized distributions of RMSD values between the starting and end conformations during SMD simulations. RMSD values were calculated based on the C_α atoms of secondary structures of RBD. Distributions were constructed based on the 640 SMD simulations performed for SARS-CoV-2.

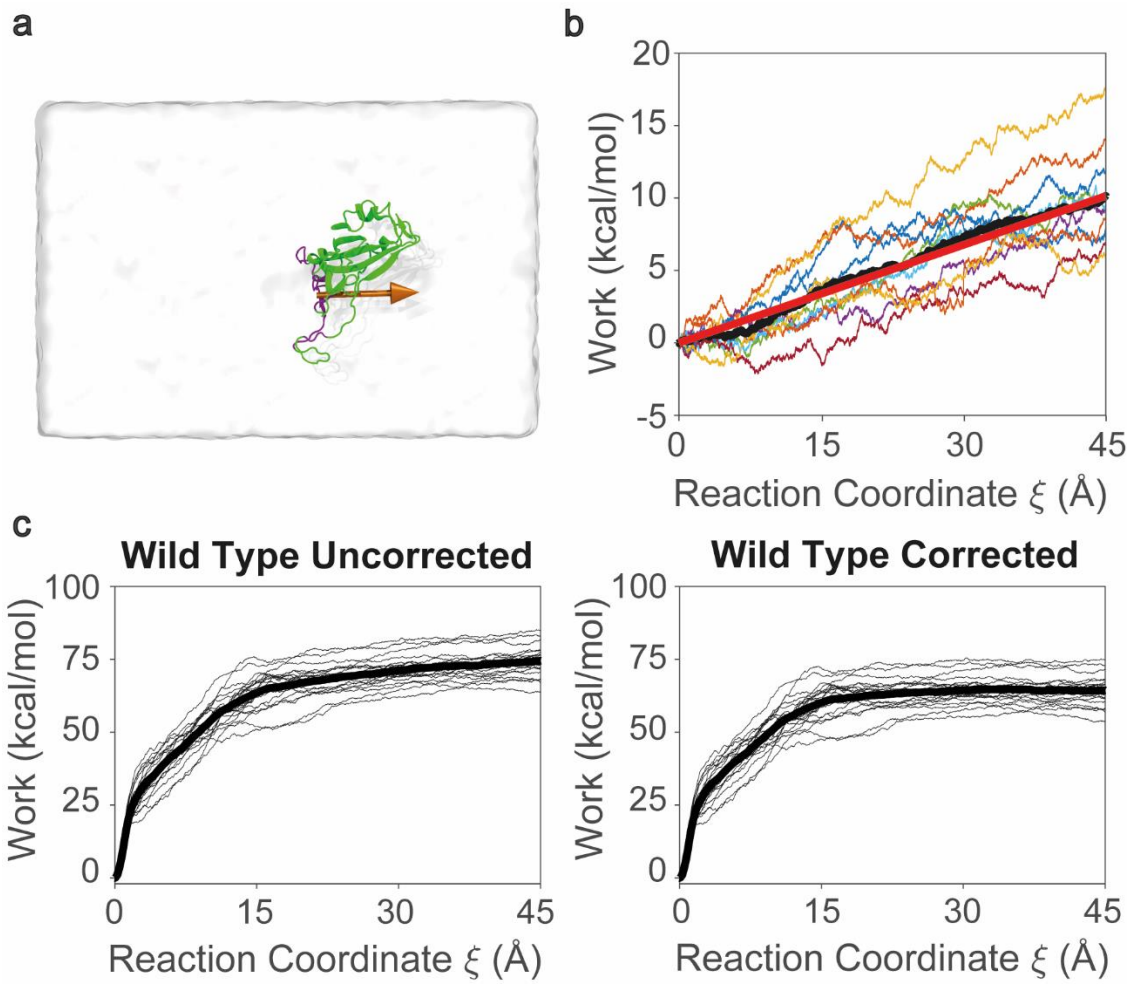


Figure S3. Work done against the viscous drag of water in SMD simulation. (a) In SMD simulations, C_α atoms of RBD (purple) were steered. The orange arrow on the RBD (green) shows the SMD pulling vector, which was taken as the reaction coordinate. (b) Work values obtained from pulling RBD in the absence of ACE2. Black line is the average work from 10 different SMD simulations. Red line represents the work done against the viscous drag of SMD simulation and was defined as the line passing through the initial and last data point of the black curve. (c) Distribution of work values are shown for uncorrected (work values as obtained from the SMD simulations) and corrected (work done against viscous drag of water is subtracted from SMD work values) are shown. Thick line represents the mean work values.

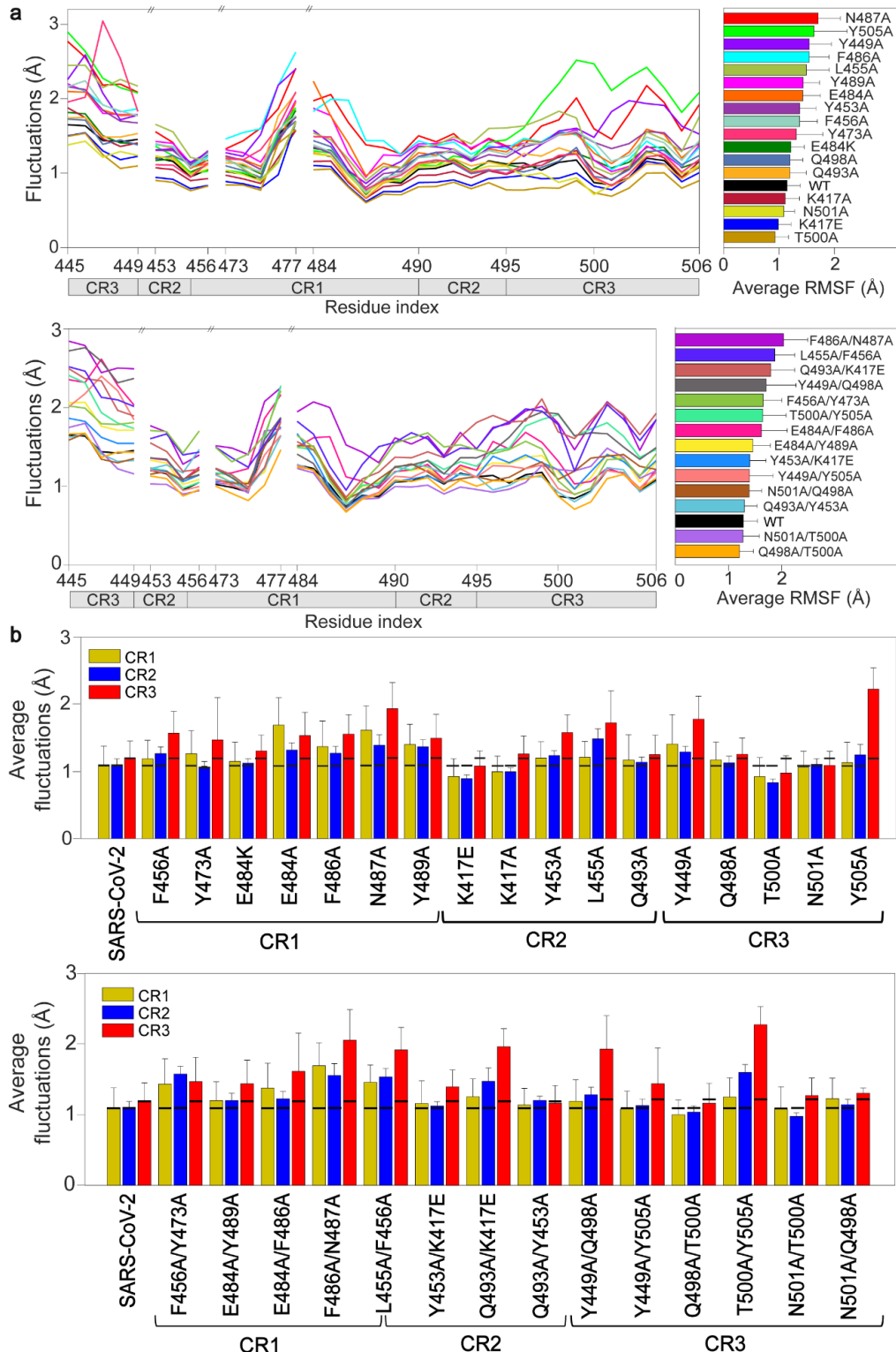


Figure S4. RMSF values of single- and double-point mutants of RBD of SARS-CoV-2. (a)

RMSF of RBD residues located on the PD binding surface of WT and point mutants. (b)

Average RMSF values of the C_α atoms at CR1, CR2, and CR3 for the WT and mutant SARS-CoV-2 RBD in complex with ACE2 PD. The black lines in each bar show the average RMSF values in CR1, CR2, and CR3 for the WT. Error bars represent s.d.

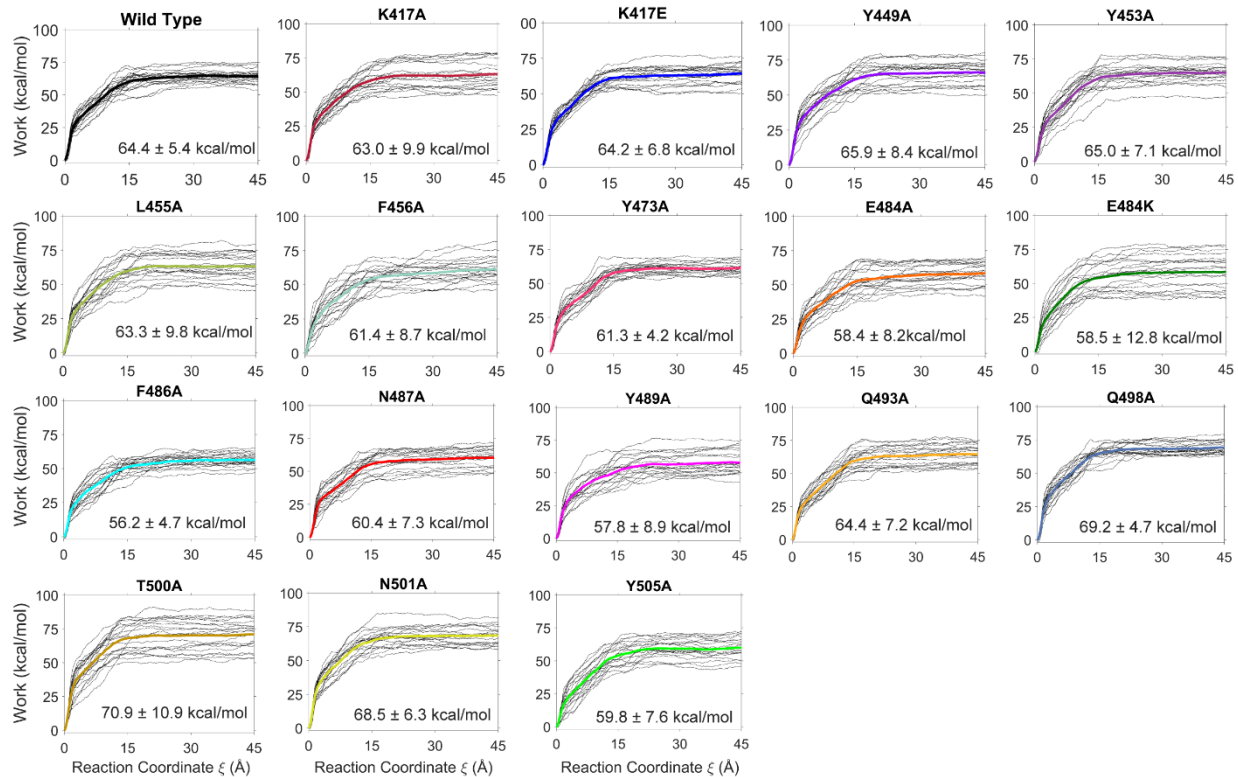


Figure S5. Distribution of work values obtained from SMD simulations for each single-point mutant system of RBD of SARS-CoV-2. Thick lines represent the average work values of each system.

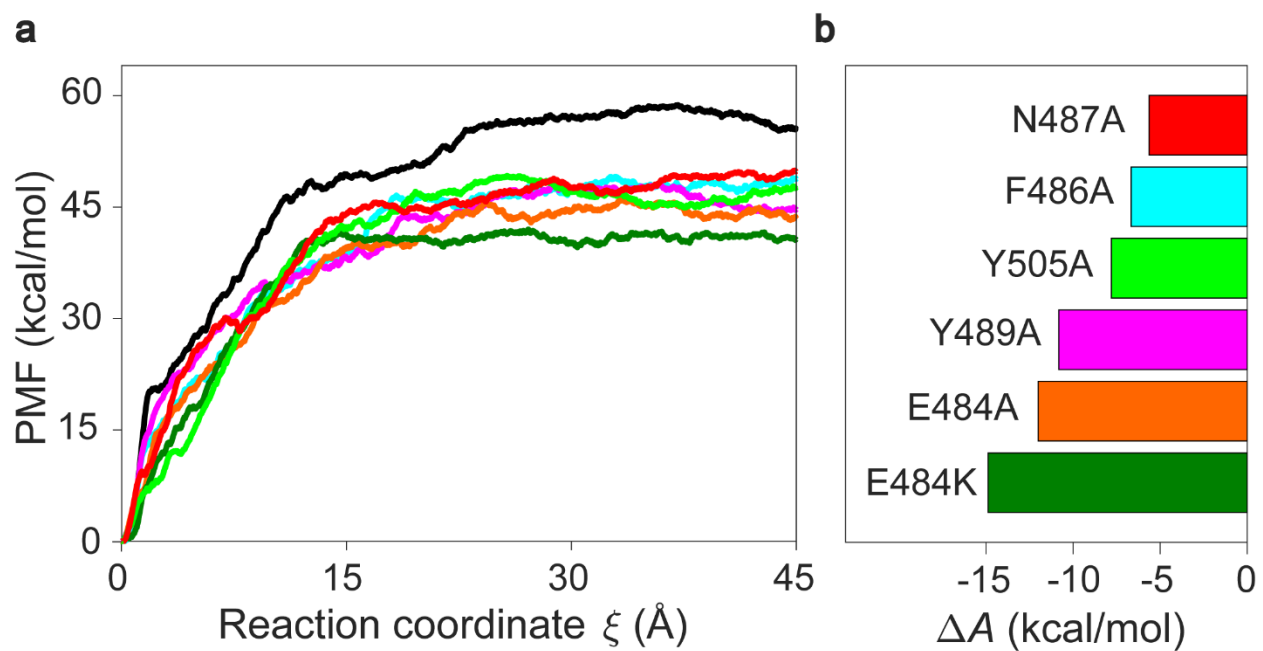


Figure S6. PMF and ΔA values of WT and six single-point mutants of RBD of SARS-CoV-2. (a) PMF values of WT and 6 single point mutants with lowest unbinding work values. (b) ΔA values of these mutants are calculated from Jarzynski equality.

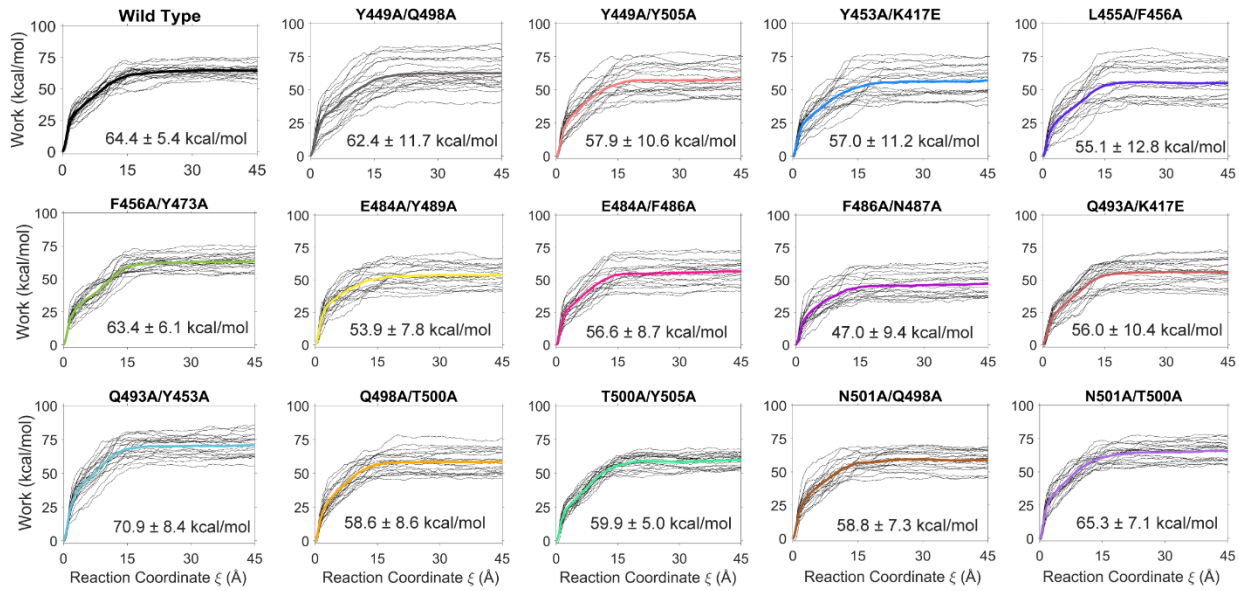


Figure S7. Distribution of work values obtained from SMD simulations for each double point mutant system of RBD of SARS-CoV-2. Thick lines represent the average work values of each system.

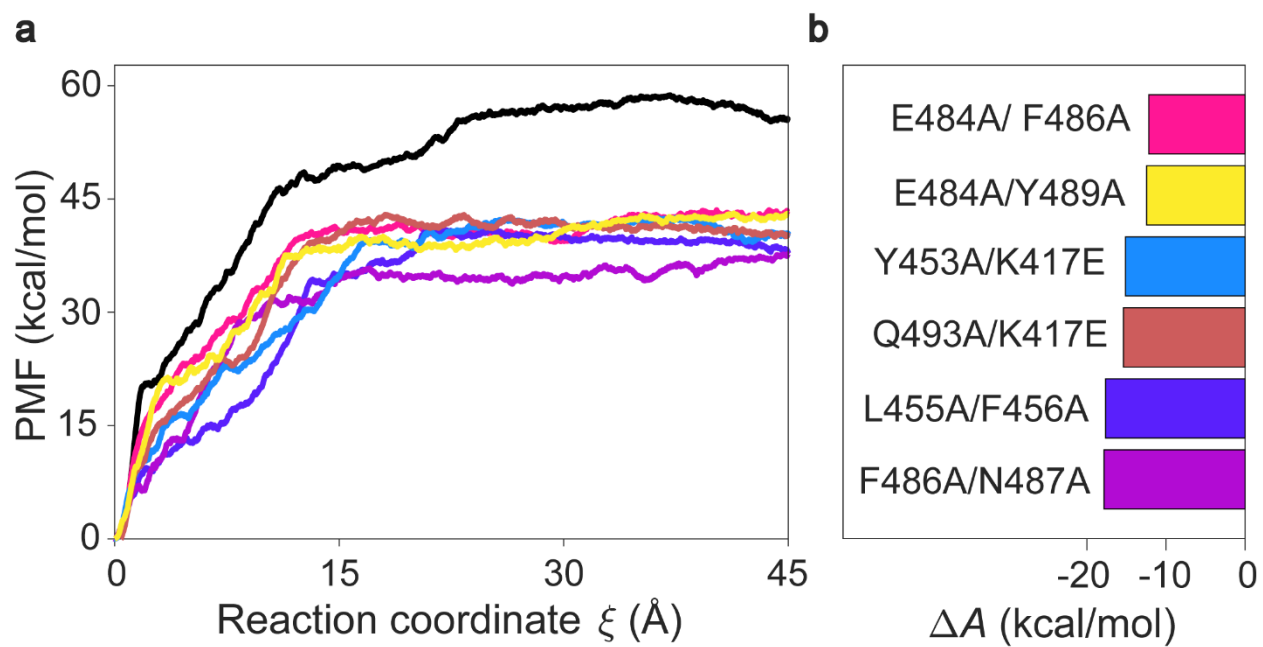


Figure S8. PMF and ΔA values of WT and six double point mutants of RBD of SARS-CoV-2. (a) PMF values of WT and 6 double point mutants with lowest unbinding work values. (b) ΔA values of these mutants are calculated from Jarzynski equality.

Table S1. Starting conformations and durations of the MD simulations performed.

Run ID	Initial state	RBD sequence	Simulation Type	Simulation Duration (ns)
1a-b	RBD-ACE2 complex (6M0J)	WT SARS-CoV-2	MD	(a) 100, (b) 100
1c-d	Final conformers of MD 1a-b	WT SARS-CoV-2	SMD	(c) 225, (d) 225
2a-b	RBD-ACE2 complex (6M0J)	K417A	MD	(a) 100, (b) 100
2c-d	Final conformers of MD 2a-b	K417A	SMD	(c) 225, (d) 225
3a-b	RBD-ACE2 complex (6M0J)	K417E	MD	(a) 100, (b) 100
3c-d	Final conformers of MD 3a-b	K417E	SMD	(c) 225, (d) 225
4a-b	RBD-ACE2 complex (6M0J)	E484A	MD	(a) 100, (b) 100
4c-d	Final conformers of MD 4a-b	E484A	SMD	(c) 225, (d) 225
5a-b	RBD-ACE2 complex (6M0J)	E484K	MD	(a) 100, (b) 100
5c-d	Final conformers of MD 5a-b	E484K	SMD	(c) 225, (d) 225
6a-b	RBD-ACE2 complex (6M0J)	Y489A	MD	(a) 100, (b) 100
6c-d	Final conformers of MD 6a-b	Y489A	SMD	(c) 225, (d) 225
7a-b	RBD-ACE2 complex (6M0J)	N487A	MD	(a) 100, (b) 100
7c-d	Final conformers of MD 7a-b	N487A	SMD	(c) 225, (d) 225
8a-b	RBD-ACE2 complex (6M0J)	F486A	MD	(a) 100, (b) 100
8c-d	Final conformers of MD 8a-b	F486A	SMD	(c) 225, (d) 225
9a-b	RBD-ACE2 complex (6M0J)	Y505A	MD	(a) 100, (b) 100
9c-d	Final conformers of MD 9a-b	Y505A	SMD	(c) 225, (d) 225
10a-b	RBD-ACE2 complex (6M0J)	Q453A	MD	(a) 100, (b) 100
10c-d	Final conformers of MD 10a-b	Q453A	SMD	(c) 225, (d) 225
11a-b	RBD-ACE2 complex (6M0J)	T500A	MD	(a) 100, (b) 100
11c-d	Final conformers of MD 11a-b	T500A	SMD	(c) 225, (d) 225
12a-b	RBD-ACE2 complex (6M0J)	Y449A	MD	(a) 100, (b) 100
12c-d	Final conformers of MD 12a-b	Y449A	SMD	(c) 225, (d) 225
13a-b	RBD-ACE2 complex (6M0J)	Q493A	MD	(a) 100, (b) 100
13c-d	Final conformers of MD 13a-b	Q493A	SMD	(c) 225, (d) 225
14a-b	RBD-ACE2 complex (6M0J)	Q498A	MD	(a) 100, (b) 100
14c-d	Final conformers of MD 14a-b	Q498A	SMD	(c) 225, (d) 225
15a-b	RBD-ACE2 complex (6M0J)	N501A	MD	(a) 100, (b) 100
15c-d	Final conformers of MD 15a-b	N501A	SMD	(c) 225, (d) 225
16a-b	RBD-ACE2 complex (6M0J)	L455A	MD	(a) 100, (b) 100
16c-d	Final conformers of MD 16a-b	L455A	SMD	(c) 225, (d) 225
17a-b	RBD-ACE2 complex (6M0J)	F456A	MD	(a) 100, (b) 100
17c-d	Final conformers of MD 17a-b	F456A	SMD	(c) 225, (d) 225

18a-b	RBD-ACE2 complex (6M0J)	Y473A	MD	(a) 100, (b) 100
18c-d	Final conformers of MD 18a-b	Y473A	SMD	(c) 225, (d) 225
19a-b	RBD-ACE2 complex (6M0J)	F486A/N487A	MD	(a) 100, (b) 100
19c-d	Final conformers of MD 19a-b	F486A/N487A	SMD	(c) 225, (d) 225
20a-b	RBD-ACE2 complex (6M0J)	E484A/Y489A	MD	(a) 100, (b) 100
20c-d	Final conformers of MD 20a-b	E484A/Y489A	SMD	(c) 225, (d) 225
21a-b	RBD-ACE2 complex (6M0J)	E484A/F486A	MD	(a) 100, (b) 100
21c-d	Final conformers of MD 21a-b	E484A/F486A	SMD	(c) 225, (d) 225
22a-b	RBD-ACE2 complex (6M0J)	T500A/Y505A	MD	(a) 100, (b) 100
22c-d	Final conformers of MD 22a-b	T500A/Y505A	SMD	(c) 225, (d) 225
23a-b	RBD-ACE2 complex (6M0J)	Y453A/K417E	MD	(a) 100, (b) 100
23c-d	Final conformers of MD 23a-b	Y453A/K417E	SMD	(c) 225, (d) 225
24a-b	RBD-ACE2 complex (6M0J)	Q493A/Y453A	MD	(a) 100, (b) 100
24c-d	Final conformers of MD 24a-b	Q493A/Y453A	SMD	(c) 225, (d) 225
25a-b	RBD-ACE2 complex (6M0J)	Q493A/K417E	MD	(a) 100, (b) 100
25c-d	Final conformers of MD 25a-b	Q493A/K417E	SMD	(c) 225, (d) 225
26a-b	RBD-ACE2 complex (6M0J)	Y449A/Q498A	MD	(a) 100, (b) 100
26c-d	Final conformers of MD 26a-b	Y449A/Q498A	SMD	(c) 225, (d) 225
27a-b	RBD-ACE2 complex (6M0J)	Y449A/Y505A	MD	(a) 100, (b) 100
27c-d	Final conformers of MD 27a-b	Y449A/Y505A	SMD	(c) 225, (d) 225
28a-b	RBD-ACE2 complex (6M0J)	Q498A/T500A	MD	(a) 100, (b) 100
28c-d	Final conformers of MD 28a-b	Q498A/T500A	SMD	(c) 225, (d) 225
29a-b	RBD-ACE2 complex (6M0J)	N501A/T500A	MD	(a) 100, (b) 100
29c-d	Final conformers of MD 29a-b	N501A/T500A	SMD	(c) 225, (d) 225
30a-b	RBD-ACE2 complex (6M0J)	N501A/Q498A	MD	(a) 100, (b) 100
30c-d	Final conformers of MD 30a-b	N501A/Q498A	SMD	(c) 225, (d) 225
31a-b	RBD-ACE2 complex (6M0J)	L455A/F456A	MD	(a) 100, (b) 100
31c-d	Final conformers of MD 31a-b	L455A/F456A	SMD	(c) 225, (d) 225
32a-b	RBD-ACE2 complex (6M0J)	F456A/Y473A	MD	(a) 100, (b) 100
32c-d	Final conformers of MD 32a-b	F456A/Y473A	SMD	(c) 225, (d) 225
33a-b	RBD-ACE2 complex (6M0J)	WT SARS-CoV	MD	(a) 100, (b) 100
33c-d	Final conformers of MD 33a-b	WT SARS-CoV	SMD	(c) 225, (d) 225
34c-d	Final conformers of MD 1a-b	WT SARS-CoV-2	SMD	(c) 300, (d) 600
35c-d	Final conformers of MD 33a-b	WT SARS-CoV	SMD	(c) 300, (d) 600